Design of intumescent fire protection for concrete filled structural hollow sections

Design of intumescent fire protection for concrete filled structural hollow sections

David Rush[1]*, Luke Bisby[1], Martin Gillie[1], Allan Jowsey[2] and Barbara Lane[3]

[1] BRE Centre for Fire Safety Engineering, University of Edinburgh, Edinburgh, UK
[2] International Paint Ltd, AkzoNobel, Newcastle, UK
[3] Arup, London, UK

Abstract

Design of intumescent protection systems for concrete filled structural steel hollow (CFS) sections in the UK typically requires three input parameters in practice: (1) a required fire resistance rating; (2) and 'effective' section factor; and (3) a limiting steel temperature for the hollow structural section. While the first of these inputs is generally prescribed in building codes, the latter two require greater engineering knowledge and judgement. This paper examines results from standard furnace tests on 26 CFS sections, 14 of which were protected with intumescent coatings by application of current UK design guidance. The protected sections demonstrate highly conservative fire protection under standard fire exposure, a conservatism not typically observed for protected unfilled steel hollow sections. The possible causes of the observed conservatism are discussed, and it is demonstrated that the method currently used to calculate the effective section factor for protected CFS columns is based on a false presumption that both unprotected and protected CFS columns can be treated in the same manner. A conservative method for determination of the steel limiting temperature for CFS columns is proposed; this can be applied by designers to more efficiently specify intumescent fire protection for CFS members.

Keywords: Composite columns, intumescent fire protection, forensic analysis, section factor, limiting temperature, design.

* Corresponding Author. e-mail address: d.rush@ed.ac.uk, Phone number: +44 (0)131 650 7241, Address: John Muir Building, Room 1.5, BRE Centre for Fire Safety Engineering, University of Edinburgh, Kings Buildings, Mayfield Road, Edinburgh, UK, EH9 3JL.

Nomenclature

A_i	area (mm^2)	t_s	steel tube thickness (mm)
b_i	internal breadth (mm)	t_{se}	effective steel thickness (mm)
c_i	specific heat capacity (J/kg^{o}C)	***Greek***	
d_p	dry film thickness (DFT) (mm)	Δt	time step (secs)
$\dot{h}_{net}$	net heat flux (W/m^2)	η	concrete core efficiency factor
H_p	heated perimeter (mm)	θ_i	temperature (^{o}C)
H_p/A_{eff} *(Th)*	current effective section factor (m^{-1})	$\lambda_{p,t}$	thermal conductivity of coating (W/m^{o}C)
H_p/A_{eff} *(exp)*	new effective H_p/A (m^{-1})	ρ_i	density (kg/m^3)
$(H_p/A_{eff})'$	instantaneous effective H_p/A (m^{-1})	***Subscripts***	
$(H_p/A_{eff})'_{(Eq.Area)}$	equivalent area effective H_p/A (m^{-1})	*s*	steel tube
$(H_p/A_{eff})'_{t,ave}$	time averaged effective H_p/A (m^{-1})	*c*	Concrete
t_{ce}	equiv. thickness from concrete (mm)	*eff*	Effective
t_{FR}	required fire resistance (mins)		

1 Introduction

Architects and engineers increasingly specify concrete filled steel hollow structural sections (CFS) in the design and construction of multi-storey buildings. A CFS sections consist of hollow steel sections that are in-filled with concrete to provide, through composite action, superior load carrying capacity and structural fire resistance as compared with unfilled steel tubes. CFS sections are an attractive, efficient, and sustainable means by which to design and construct compressive members in highly optimized structural frames. The concrete infill and the steel tube work together, at both ambient temperatures and during fire, yielding several benefits: the steel tube acts as stay-in-place formwork during casting of the concrete, thus reducing forming and stripping costs, and provides a smooth, rugged, architectural surface finish; the concrete infill enhances the steel tube's resistance to local buckling; and the steel tube sheds axial load to the concrete core (whether reinforced or unreinforced) when heated during a fire, thus enhancing the fire resistance of the column [1].

Multi-storey buildings often require structural fire resistance ratings of two hours or more [2], which CFS sections can provide without the need for applied fire protection in some cases. However where the structural fire design guidance [1, 3-6] shows that adequate fire resistance is unachievable, external fire protection must be applied to the steel tube; in the UK the preferred method of fire protection is often intumescent coating.

In practice, the design of intumescent fire protection systems for CFS sections requires an assumed (typically prescribed) limiting steel temperature at some predefined (also prescribed) period of standard fire exposure. This is a difficult task for three reasons. Firstly, there is a paucity of test data on the performance of intumescent coatings when applied on CFS sections due to the sensitive and unique composition of each specific intumescent coating product. Secondly, quantifiably observing the comparatively complex thermal response of intumescent coatings during fire resistance tests in furnaces is difficult. Intumescent fire protection coatings expand up to 100 times their original thickness [7] when exposed to heat by creating a fragile multi-cellular protective insulating layer, which is unique to the heating rate, chemical composition and the initially applied dry film thickness (DFT) of the coating. Lastly, fundamental differences exist between the evolution of thermal gradients within protected, as opposed to unprotected, CFS sections.

This paper assesses current fire resistant design guidance for intumescent fire protection systems applied on CFS sections in the UK, examining the prescription methods for DFTs on CFS sections and identifying the causes of conservative outcomes observed in a series of furnace tests on both protected and unprotected CFS columns; also presented herein. A conservative method to prescribe the design limiting steel temperature for protected CFS columns is suggested, and data and discussions supporting the ongoing development of rational, performance-based approaches to the structural fire design of CFS columns is given.

2 Specification of intumescent coatings for CFS sections

Design of intumescent fire protection (i.e. design DFTs) applied to structural steel is typically based on three input parameters: (1) the required *fire resistance*, F.R., which is typically a prescribed value based on local building code requirements (e.g. [2]) and is generally dependent on the type, height, and design of the building; (2) a *section factor,* defined as the

ratio of the section's heated perimeter, H_p, to its cross sectional area, A; and (3) the assumed *limiting temperature* of the steel, which is the temperature at which the steel is presumed to fail under load during a standard furnace test (in most cases this is close to 520°C). Engineers use these three input parameters in conjunction with empirically determined, product specific, design tables to determine the required DFT of the specific intumescent coating needed to maintain the critical temperature of the steel below its critical temperature for the required duration of standard fire exposure. The product specific design tables are based on numerous large scale furnace tests on plain structural steel sections with various H_p/A values and at a variety of DFTs.

To apply existing DFT tables for protection of CFS sections without the need to perform a very large number of furnace tests, an 'effective' section factor, H_p/A_{eff}, must be determined; this must incorporate the effect(s) of the concrete infill on the heating rates of the steel and on the load bearing capacity of the composite column. Equations 1 and 2 represent the current approach to determining the effective section factor for CFS sections [8] in the UK; this is based primarily on the required fire resistance time, t_{FR}. Equations 1 and 2 treat the problem by using DFT design guidance developed for unfilled steel sections but add an 'equivalent' steel wall thickness, t_{ce} , which is dependent on the internal breadth of the section, b_i, and t_{FR}, to the existing steel wall thickness, t_s, to account for the thermal sink effects of the concrete core, thus decreasing the effective H_p/A:

$$\frac{H_p}{A_{eff}} = \frac{1000}{t_{se}} = \frac{1000}{t_s + t_{ce}} \tag{1}$$

$$t_{ce} = \begin{cases} 0.15 b_i, & b_i < 12\sqrt{t_{FR}} \\ 1.8\sqrt{t_{FR}}, & b_i \geq 12\sqrt{t_{FR}} \end{cases} \tag{2}$$

This approach seems physically unrealistic and thus limited (and potentially flawed) on a number of grounds, as discussed below. Neither the physical rationale nor the theoretical or empirical basis for Equation 2 are clear (or reported in the literature), and therefore a further

objective of the research presented herein was to validate (or otherwise) this approach. Regardless, this is the current approach that is applied on real projects in the UK.

3 Furnace tests on unprotected and protected CFS sections

To evaluate and improve the performance of the above approach for prescribing dry film thicknesses for the fire protection of CFS sections, twenty-six CFS columns, 14 protected and 12 unprotected, were exposed to the ISO-834 [9] standard fire in a fire testing furnace for 120 minutes, as outlined in Table 1 (one exception was a single specimen that was heated for a total duration of 180 minutes, as described below). The waterborne intumescent coating dry film thicknesses (DFT) for the 14 protected CFS sections in Table 1 was prescribed using effective H_p/A values given by Equation 1 with a presumed limiting steel temperature of 520^{o}C and a required F.R. of 90 minutes. Exceptions were that one specimen was designed to a F.R. of 75 minutes (and tested for 120 minutes) and one was protected for 120 minutes F.R. (tested for 180 minutes). A schematic of typical test specimen layouts is given in Figure 1.

Cross-sectional temperatures were recorded at two heights during testing, as shown in Figure 1. Four K-Type thermocouples measured steel tube temperatures and one K-Type thermocouple measured concrete core temperatures at the centre of the cross-section at both sections. The majority of tests were conducted in a 4 m × 3 m × 2 m ceramic tile lined full scale floor furnace in which gas temperatures were monitored using six thermocouples. The two protected specimens with DFTs designed for 75 and 120 minutes fire resistance (tests 23 and 24 in Table 1) were tested in a smaller 1.8 m × 1.8 m × 1.8 m ceramic tile lined cube furnace in which temperatures were monitored with three thermocouples. All specimens were constructed from Grade S355 structural steel sections and filled with a hybrid steel and polypropylene (PP) fibre reinforced concrete mix incorporating 40 kg/m^3 and 2 kg/m^3 of steel and PP fibres, respectively, with a compressive strength of between 46.1 and 59.4 MPa and a

moisture content between 3% and 6% by mass at the time of testing. Full details of the tests, including residual (post-heating) structural tests to failure, are presented in [10].

4 Results and discussion

Table 1 shows the average steel tube (eight thermocouples) and concrete core (two thermocouples) temperatures observed at 90 minutes and 120 minutes during fire testing. The data unsurprisingly show that the temperature difference between the steel tube and the centre of the concrete is much greater in unprotected sections than in those with protection. As expected, thermal gradients in protected CFS sections are much less severe, for the same steel tube temperature, than those in unprotected CFS sections. The data also show that the observed steel temperatures in the protected sections are well below the target design limiting temperature of 520^{o}C at the required F.R. time (90 minutes unless otherwise noted in Table 1). For instance, the maximum temperature experienced by any of the steel tubes protected to 90 minutes at 90 minutes of exposure was 265^{o}C, a full 255^{o}C less than the design limiting temperature of 520^{o}C. Finally, Table 1 shows that the size of the concrete core affects the temperatures observed within the steel tube; with lower steel temperatures observed for CFS sections with proportionally larger cores.

Figure 2 shows the average, maximum, and minimum observed steel tube temperatures, θ_s, for all unprotected and protected tests (excluding tests 23 and 24). It is clear from this figure (and from Table 1) that use of current guidance and DFT design data from unfilled steel sections to prescribe DFTs for CFS sections results in highly conservative steel tube temperatures during standard furnace testing. The limiting temperature was never reached; only tests 23 and 24 experienced temperatures greater than the prescribed 520^{o}C, and in both cases this occurred more than 30 minutes after the required F.R. time had been met. Thus, if

current guidance is used to prescribe DFTs for CFS sections excessive amounts of fire protection will be applied; while conservative this is clearly non optimal.

The observed conservatism in the test data could be due to: (1) inherently conservative DFT thicknesses in the tabulated data from tests on unfilled sections; (2) changes in the expansion response and thus the effective thermal conductivity of the intumescent coatings when applied to sections with very different thermal masses; or (3) incorrect or unrealistic calculation of the effective section factors for CFS sections.

The product specific tabulated DFTs, available from reactive coating manufacturers and based on numerous fire tests of their products, are already highly optimised for the case of protecting unfilled steel sections. A large number of furnace tests have shown that in most cases the designed limiting temperatures, upon which the DFTs for design are based, are indeed typically reached at, or shortly after, the required F.R. times for protected unfilled sections. For instance, a 219 × 16 mm Ø circular hollow section and a 200 × 200 × 6.3 mm square hollow section, designed for fire resistances of 90 and 120 minutes, respectively, both reached a limiting temperature of 520^{o}C, at 92 and 123 minutes respectively, in standard furnace tests. Thus, inherently conservative design tables for the plain steel sections (Cause (1) above) are not likely to be the cause of the observed conservatism in Figure 2.

4.1 Variable thermal conductivity of protection

The authors assessed the variable effective thermal conductivity of the intumescent protection according to guidance presented in BS EN 13381-8 [11], to investigate whether the conservatism seen in the observed temperatures was due to fundamental changes in the insulating performance of the intumescent coating (i.e. its melting, foaming, and charring processes) for substrates of significantly different thermal mass (i.e. filled versus unfilled steel hollow sections). In practice, the determination of both the applied dry film thickness (DFT, d_p) and effective variable thermal conductivity use section factors (effective or

otherwise), with the latter also using DFTs, as input variables. Therefore it is reasonable to compare the effective thermal conductivities of filled and unfilled hollow sections (acknowledging that section factors for filled and unfilled tubes of the same size are not the same and neither are their design DFTs).

The variable thermal conductivity of the protection was calculated in accordance with BS EN 13381-8 [11], for otherwise identical filled and unfilled sections, using:

$$\lambda_{p,t} = d_p \cdot \frac{A_{eff}}{H_p} \cdot c_s \cdot \rho_s \cdot \left(\frac{1}{(\theta_t - \theta_{s,t}) \cdot \Delta t} \right) \cdot \Delta\theta_{s,t} \qquad (3)$$

where $\lambda_{p,t}$ is the variable effective thermal conductivity; d_p is the protection DFT; A_{eff}/H_p is the inverse of the calculated effective section factor, H_p/A_{eff}; c_s and ρ_s are the specific heat capacity and density of steel respectively; θ_t is the furnace temperature; $\theta_{s,t}$ is the steel tube temperature; Δt is the analysis time step; and $\Delta\theta_{s,t}$ is the change in steel tube temperature during that time step.

Figure 3 shows the calculated variable effective thermal conductivity, $\lambda_{p,t}$ (Equation 3), as a function of steel tube temperature, for the intumescent protection on all of the protected CFS circular sections (circles – tests 13 to 24), and specifically for the protected 219.1 mm diameter *filled* CFS sections (tests 16 to 18). Figure 3 also shows the variation in $\lambda_{p,t}$ for the same intumescent protection applied to *unfilled* 219.1 mm Ø steel tubes, and shows that the variable thermal conductivity of the protection, when applied on filled versus unfilled hollow sections, is effectively the same.

Figure 3 shows that there is a reasonable empirical understanding of the relationship between the DFT and the section factor for this product, as shown by the similarities between the effective thermal conductivity response of the different DFTs (from 2 mm to 4 mm DFT, from tests 23 and 24), on sections with different effective section factors (H_p/A_{eff} varying from 38m^{-1} to 55m^{-1}) with different levels of design fire resistance (75, 90, 120 minutes).

This suggests that the thermal mass of the substrate has no obvious effect on the insulating response of the intumescent coating when subjected to a standard cellulosic fire curve in a testing furnace, and therefore that the conservatism in the prescription of DFTs is unlikely to be a result of Cause (2), postulated previously.

4.2 'Effective' section factors for CFS sections

Equation 2 gives the method currently used in the UK to artificially account for the changes in effective section factor of a CFS section resulting from infilling with concrete; its application for specifying DFTs for protected CFS sections results in lower than expected steel temperatures in full scale furnace tests (refer again to Figure 2). As discussed, this conservatism is not due to either an inherent conservatism in the tabulated DFT data used to specify intumescent protection thickness (Cause (1)), nor to differences in the thermal performance of the intumescent on substrates of different thermal mass (Cause (2)). Problems therefore lie within the calculation of effective section factor based on Eq. 2. To assess this hypothesis and determine whether improvements can be made, a discussion on the development of the current H_p/A_{eff} guidance (Eq. 2) is necessary, both for unprotected and protected CFS sections, using new experimental data from the tests listed in Table 1.

4.2.1 Development of current guidance

The existing H_p/A_{eff} guidance given in Eqs. 1 and 2 [8] assumes that:

1. CFS sections can be treated as hollow steel tubes in which the concrete core provides an equivalent additional thickness of steel wall, using an empirical equation based on its required fire resistance time; and
2. the effective section factor for unprotected CFS sections can be determined in the same manner as protected CFS sections, as for protected versus unprotected unfilled sections.

Edwards [12] used these two assumptions to develop Eqs. 1 and 2 and assumed that the increase in steel temperature for an unprotected steel hollow section, or for a CFS section

where the concrete is converted into an equivalent thickness of steel, can be calculated using a simple energy balance, for example from BS EN 1993-1-2 [13]:

$$\Delta\theta_{s,t} = \frac{\dot{h}_{net}}{c_s \cdot \rho_s} \cdot \frac{H_p}{A} \cdot \Delta t \tag{4}$$

where the increase in steel temperatures, $\Delta\theta_{s,t}$, during a time interval, Δt, is determined based on the section factor, H_p/A, the net heat flux, $\dot{h}_{net}$, and the thermal capacity of the steel, $c_s \cdot \rho_s$. Edwards [12] used data from six standard furnace tests on unprotected CFS columns to determine an *instantaneous* effective section factor, $H_p/A_{eff}\ (exp)$, at each instant in time, by rearranging Eq. 4, giving:

$$\frac{H_p}{A_{eff}}(\exp) = \frac{\Delta\theta_{s,t} \cdot c_s \cdot \rho_s}{\dot{h}_{net} \cdot \Delta t} \tag{5}$$

where the density of steel is taken as $\rho_s = 7850$ kg/m^3. The specific heat of steel is taken as $c_s = 473 + 20.1 \cdot (\theta_s/100) + 3.81 \cdot (\theta_s/100)$ up to a temperature of 800^{o}C, after which a constant value of 877.6 J/kg·K is assumed by Edwards [12].

Edwards [12] also uses the BS EN 1991-1-2 [14] method for calculating $\dot{h}_{net}$, where the net heat flux is the summation of the radiative and convective heat fluxes. However, in determining the radiative heat flux, Edwards assumes a resultant emissivity (i.e. the combined fire emissivity ε_f, and steel emissivity, ε_s) of 0.32 without a clear justification. It is important to note that in determining the instantaneous effective section factor from furnace experiments using the equations described above, low values of the resultant emissivity will result in lower net heat flux and thus larger instantaneous effective section factors being calculated (this is assumed to be conservative from a design perspective).

In calculating the instantaneous effective section factor, $H_p/A_{eff}\ (exp)$, from test data, Edwards [12] found that the effect of the concrete core varied with time during a furnace test. This is in contrast with unfilled steel sections in which the section factor remains constant for the duration of a fire test. Clearly, this is because steep thermal gradients develop within the

concrete infill in an unprotected CFS section; in an unfilled section the high thermal conductivity of steel results in a nearly uniform temperature profile throughout the section. Using the calculated experimental instantaneous effective section factors Edwards [11] calculated the apparent instantaneous thickness of the steel tube, t_{se}, at every instant in time during fire exposure, and then determined the apparent effective increase in the steel tube thickness resulting from the presence of the concrete core, t_{ce}. How this was used to develop the specific correlations given in Eq. 2 is neither clear nor available in the literature.

4.2.2 H_p/A_{eff} *(exp)* for unprotected CFS sections

Using the same process as Edwards [12] (i.e. Eq. 5), it is possible to calculate the instantaneous H_p/A_{eff} *(exp)* for the 12 unprotected CFS sections tested in the current study and detailed in Table 1. To calculate H_p/A_{eff} *(exp)* an experimental net heat flux is required. A separate finite element heat transfer analysis [10] found that an assumed furnace emissivity of 0.38 was required to properly model the heat transfer during the tests on the unprotected CFS sections listed in Table 1, and that a temperature dependent emissivity of steel based on tests conducted by Paloposki and Liedquist [15] was the most appropriate modelling choice for accurate thermal simulations of the unprotected furnace tests presented herein. The resultant emissivity was thus assumed to vary with temperature between 0.08 for steel temperatures of 20-350^{o}C, increasing to 0.25 at 565^{o}C, and constant at 0.25 above 565^{o}C. The temperature dependent specific heat capacity of steel was assumed based on BS EN 1993-1-2 [13].

Figure 4(a) shows a representative comparison of the calculated instantaneous H_p/A_{eff} *(exp)* using Eq. 5 and Edwards' [10] theoretical H_p/A_{eff} *(Th)* (Eq. 1) for a typical unprotected CFS section (Test 4 of Table 1 in this case). The mild peak highlighted with a data marker in the H_p/A_{eff} *(exp)* curve coincides with a phase change in the steel at 735^{o}C which causes a spike in the specific heat capacity of the steel; this was seen for all of the unprotected tests. Also common to all unprotected tests was the considerable variability in calculated

instantaneous H_p/A_{eff} *(exp)* during the first 30 minutes of heating. This is due to the imperfect, variable control of the furnace temperatures and the large differences between the steel and furnace temperatures during the early stages of heating; this created large swings in the apparent net heat flux during each 60 second interval and thus in the calculated instantaneous effective H_p/A_{eff} *(exp)* values.

Figure 4(b) shows the instantaneous H_p/A_{eff} *(exp)* values determined for all unprotected sections listed in Table 1, calculated at ten minute intervals throughout the tests (data markers). This figure shows that the values of the averaged instantaneous H_p/A_{eff} *(exp)* based on the wall thicknesses are, with notable exceptions before 60 minutes of fire exposure, slightly lower at a given fire exposure time than Edwards' H_p/A_{eff} *(Th)*. However, Edwards' equation (Eq. 1) is a reasonable predictor of the overall trends observed in the data. Figure 4(b) also shows that the 'effective' contribution of the concrete core varies with time, as also noted by Edwards [12]. Clearly, this is due to the comparably low thermal conductivity of the concrete core which results in steep thermal gradients in the unprotected CFS sections that would not exist in hollow steel tubes. Larger concrete cores have more pronounced thermal gradients, as seen in Table 1, and these persist for longer durations of fire exposure. The contribution of the concrete core thus also depends on the dimensions of the concrete core, a factor for which Edwards' guidance fails to account.

4.2.3 Concrete core size and theoretical effective H_p/A_{eff} values

To calculate the instantaneous H_p/A_{eff} for unprotected CFS sections in a physically realistic manner the effect of the concrete thermal gradients and core size need to be incorporated. Equation 6 below proposes a new method to calculate the instantaneous section factor, (H_p/A_{eff})', by converting the concrete core into an equivalent *area* of steel based on the size of the core, A_c, the ratio of the respective heat capacities of concrete and steel ($c_c \cdot \rho_c$ and $c_s \cdot \rho_s$ for concrete and steel, respectively), and an empirically determined concrete core efficiency

factor, η. The ratio of thermal properties has no physical meaning, however it is shown below to result in a useful empirical correlation that is applied later in this section. Using the instantaneous H_p/A_{eff} *(exp)* calculated on the basis of the tests in Table 1 as inputs into Eq. 6 (i.e. H_p/A_{eff} *(exp)* = (H_p/A_{eff})'), values of the concrete core efficiency factor, η, can be calculated during each time interval as follows:

$$\left(\frac{H_p}{A_{eff}}\right)' = \frac{H_p}{A_S + \eta \cdot \frac{(c_c \cdot \rho_c)}{(c_s \cdot \rho_s)} \cdot A_c} \tag{6}$$

where c_c = 1000 J/kg^{o}C , ρ_c = 2300 kg/m^3, c_s is the temperature dependent relationship described in Section 3.3.1 (4) of EC4 [4] to account for the phase change in steel, and ρ_s = 7850 kg/m^3.

Figure 5 shows the variation of η with time for two representative unprotected CFS sections exposed to an ISO-834 [9] standard fire, and shows that the relationship between η and the furnace time, t_{furn}, is approximately linear, however with considerable variability. The variability in η is due to the measured steel and furnace temperature changes being small and measured with a resolution of only 1°C at 60 second intervals. The result of this is highlighted for example by the three points (white circles) in Figure 5(a) where the steel temperature change between minutes 103-104-105-106 is 3-1-4^{o}C, respectively. The precision of the temperature data acquisition 1^{o}C, and is a result of as the K-type thermocouples used have a precision of ±2^{o}C, so data are recorded at a coarseness of less than 1^{o}C would be rather difficult to defend. In any case, the trend in the data of Figure 5 is reasonably clear.

As with Edwards' [12] calibration of effective wall thickness (Eq. 2), the apparent efficiency of the concrete core, η, varies with time of fire exposure. If it is assumed that the relationship between η and fire exposure time, t_{furn}, is linear, then a larger gradient of η/t_{furn} is

found for smaller internal breadths of concrete, as expected given that smaller cores have less thermal mass and will heat up more rapidly.

Figure 6 plots η with respect to fire exposure time, t_{furn}, for all unprotected square and circular sections listed in Table 1. Figure 6 shows that as the breadth of a CFS column increases, and hence so does the size of the internal concrete core, the assumed linear gradient η/t_{furn} decreases. The internal breadth, b_i, of a CFS section can be compared to the gradient η/t_{furn}, as shown in Figure 7, to give a relationship for η/t_{furn} for both square and circular sections based on the internal breadth of the concrete core.

The relationships shown in Figure 7 between the gradients of η/t_{furn} and the internal breadths of the CFS columns assume an inverse function. This is physically realistic since η must always remain positive and decreases as the core size increases. The calculation of η can thus be expressed in terms of the internal breadth, b_i, and time of furnace exposure, t_{furn}, as:

$$\eta = \begin{cases} 0.0080 \cdot b_i^{-0.53} \cdot t_{furn} & Circular \\ 0.0038 \cdot b_i^{-0.96} \cdot t_{furn} & Square \end{cases} \quad (7)$$

Instantaneous theoretical (H_p/A_{eff})' values can then be calculated with respect to time using η values calculated from Eq. 7, with an iterative process involving the calculation of the change in steel temperature using Eq. 3. Figure 8 compares, for a representative unprotected specimen (a 219.1 Ø × 8 mm wall thickness circular section in this case), the variation of instantaneous (H_p/A_{eff})', and $H_p/A_{eff}\,(Th)$ calculated from Edwards' current guidance (Eq. 1), to the instantaneous $H_p/A_{eff}\,(exp)$ calculated from test data (Eq. 4) with respect to time; this shows that the instantaneous (H_p/A_{eff})' is an accurate and more realistic predictor of the instantaneous $H_p/A_{eff}\,(exp)$; being reasonably accurate for all of the tests. It is noteworthy that the *instantaneous* (H_p/A_{eff})' at 60 minutes is counter intuitively higher than the value at 45 minutes. This is due to a peak caused by the phase change in steel at about 735°C which increases its specific heat capacity over a small temperature range.

4.2.4 Instantaneous (H_p/A_{eff})' and design

The instantaneous (H_p/A_{eff})' calculation (Eq. 6) is a superior predictor of the observed *instantaneous* effective section factor for unprotected CFS sections during furnace exposure. However, (H_p/A_{eff})' only calculates the effective section factor values at one specific instant in time. These values are not applicable for determining the design DFT of an intumescent coating to protect a CFS section because the calculated theoretical steel temperatures based on a single instantaneous (H_p/A_{eff})' for a specific required fire resistance time are lower than those calculated with a variable (H_p/A_{eff})' calculated during each time step, as shown in Figure 9.

Figure 9 compares the experimental steel temperatures for a representative unprotected 219.1 Ø × 8 mm wall thickness circular CFS to steel temperatures calculated using Eq. 4 (with a time step of six seconds) using variable effective section factors, either (H_p/A_{eff})' or H_p/A_{eff} (Th) from Eq. 6 or Eq. 1, respectively, calculated at every time step. Figure 9 shows that the calculation of steel temperature using either the variable (H_p/A_{eff})' or H_p/A_{eff} (Th) provides reasonably accurate predictions.

Figure 9 also shows the predicted steel tube temperature at 15 minute intervals (again using Eq. 4 with a six second time step) based on a single instantaneous effective section factor calculated using either (H_p/A_{eff})' or H_p/A_{eff} (Th) from Eq. 6 or Eq. 1, respectively; these values are given in Table 2. It is clear that using a single instantaneous effective section factor under-predicts the observed steel temperatures, and that this is unconservative for structural fire resistance calculations. If the single instantaneous effective section factor values were used it would lead to design DFTs smaller than required.

The temperatures experienced by the steel tube of an unprotected CFS result from cumulative heating where the (H_p/A_{eff})' varies with time, whereas for an unprotected plain steel section the increase in temperature (Eq. 4) is based on a single value of H_p/A. It is thus

clearly inappropriate to use a single instantaneous value of (H_p/A_{eff})' to calculate either the steel temperature after a given length of time or the required DFT for protection.

4.2.5 Time-averaged effective section factor, $(H_p/A_{eff})'_{t,ave}$

As already noted, the effective section factor of a CFS column in fire varies with time due to the thermal gradients which exist within the concrete core. However, specifying intumescent coating thicknesses from tabulated DFT data requires a single effective section factor that accounts for the cumulative heating of a CFS section resulting from time dependent instantaneous (H_p/A_{eff})' values (Eq. 6). This single time-averaged effective section factor, $(H_p/A_{eff})'_{t.ave}$, must account for the cumulative heating history of the section factor so calculations of steel tube temperatures (Eq. 4) are the same when using either the single time averaged effective section factor, $(H_p/A_{eff})'_{t.ave}$, or the variable time dependent instantaneous (H_p/A_{eff})' values calculated from Eq. 6.

The determination of a single time-averaged effective section factor, $(H_p/A_{eff})'_{t.ave}$, for a CFS section first requires the derivation of the (H_p/A_{eff})' curve (e.g. as in Figure 5(b)). Using this time variable (H_p/A_{eff})' as an input to Eq. 4, the increase in steel temperature for each time step is calculated. When summed this results in the steel temperature of the tube at the required fire resistance time. A similar stepwise calculation must then be performed using a constant H_p/A_{eff} value to arrive at the same steel temperature after the same duration of fire exposure. This procedure must then be repeated for each and every fire resistance time to give a trace of $(H_p/A_{eff})'_{t.ave}$ with fire exposure time.

Figure 10(a) shows the time-averaged effective section values, $(H_p/A_{eff})'_{t.ave}$ for a representative unprotected test (the 219.1 Ø × 8 mm wall thickness circular CFS in this case), and gives a representative comparison of the instantaneous (H_p/A_{eff})' and $H_p/A_{eff}\,(exp)$ values with time of fire exposure, and the current effective section factor guidance $H_p/A_{eff}\,(Th)$ and $(H_p/A_{eff})'_{t.ave}$ values. The representative averaged areas are schematically shown for each 15

minutes for fire exposure: this process was repeated for all unprotected CFS sections in the current study, and the resulting $(H_p/A_{eff})'_{t.ave}$ values are compared to the H_p/A_{eff} (Th) values in Figure 10(b).

Figure 10(b) shows that the time-averaged effective section factors, for the unprotected CFS sections from Table 1, are generally greater than the effective section factors calculated at the same time using the current guidance, H_p/A_{eff} (Th) (Eq. 1). Therefore, if the time-averaged $(H_p/A_{eff})'_{t.ave}$ values for the unprotected CFS sections were to be used in the prescription of the dry film thickness (DFT) of an intumescent paint, a thicker DFT would be prescribed as compared to the DFT prescribed on the basis of H_p/A_{eff} (Th) for the same limiting temperature and required fire resistance.

Thicker DFTs would result in even lower steel tube temperatures for a protected CFS section than those observed in the protected tests (Figure 2), where the design DFTs were based on lower effective section factors calculated from Edwards' H_p/A_{eff} (Th). Whilst the new time-averaged $(H_p/A_{eff})'_{t.ave}$ values may be more physically realistic than Edwards' approach, they appear not to address the observed conservatism in furnace tests of protected CFS columns.

The conservatism seen in prescription of the DFTs is thus not attributable to inaccurate determination of the effective section factors for unprotected CFS sections. Rather, the conservatism results from the false assumption that the effective section factors for *unprotected* and *protected* CFS sections are the same. There are fundamental changes in the thermal gradient within a protected CFS section compared to that within an unprotected section. Protected CFS sections experience a much less severe thermal gradient within the concrete infill which effectively increases the effect that the concrete core has on the effective section factor, and so the effective section factor of similar protected and unprotected CFS sections will be very different.

The thermal gradient within a protected CFS section is dependent upon the heating rate that the steel experiences, which in turn is affected by:

1. the limiting temperature to which the steel is protected, since higher limiting temperatures result in more severe thermal gradients in the core and diminish the effect of the concrete;
2. the required fire resistance period, with longer fire resistances producing shallower thermal gradients and increasing the effect of the concrete core; and
3. the performance of the intumescent coating, especially its variable effective thermal conductivity and physical charring characteristics, with time of fire exposure.

To avoid this conservatism, which appears to be inherent in the current approach to specification of intumescent protection DFTs for CFS sections, additional analytical work and experimental testing of protected CFS sections is needed. A broad range of heating rates to the steel must be considered so that the effective section factor for protected CFS sections is better understood and a rational means of prescribing effective section factors can be developed. In the interim, the authors recommend that current guidance from Eqs. 1 and 2 [8] be used to determine the effective section factor for CFS columns, since the testing and analysis presented herein show this approach to be conservative.

4.3 Limiting steel temperature for protected CFS sections

Designing intumescent protection DFTs for CFS columns requires not only an effective section factor and required fire resistance time, but also an assumed limiting steel temperature (i.e. temperature of the steel tube at which the CFS column fail under load during a fire). It is common practice to assume a limiting value between 520^{o}C and 550^{o}C for steel hollow sections (filled or unfilled) and load levels (based on the approximate 60% of ambient capacity of plain steel sections at these temperatures). This could lead to overly conservative design DFTs.

For unfilled hollow sections, designers can calculate more accurate limiting temperatures of the steel section based on the load level applied [13]; however, for CFS sections this calculation is more complex since the concrete core, which typically carries a portion of the applied load, experiences a complex heating-rate-dependent thermal gradient. Paradoxically, for a CFS column the limiting temperature also changes with the amount of applied fire protection. Unprotected CFS columns typically experience very steep thermal gradients in the concrete core, and at the point failure the steel will generally be much hotter than the average concrete core temperature. This means that the concrete core retains a large proportion of its strength for a given steel tube critical temperature.

When fire protection is added the heating rate to the steel tube is reduced and thus the thermal gradient within the steel and concrete core becomes shallower and core temperatures more uniform. The reduced heating rate also reduces the temperature difference between the steel tube and the average concrete core temperature for a protected CFS section. Therefore for the same steel tube temperature the concrete core has comparatively lower strength in a protected CFS section as compared to a similar unprotected CFS section. This in turn reduces the limiting steel tube temperature at failure; the limiting steel tube temperatures of protected CFS sections are thus lower than those of similar unprotected CFS sections.

Predicting the limiting temperatures and structural response of protected CFS columns is difficult due to the lack of widely available and reliable variable thermal properties for intumescent coatings. In the absence of more detailed knowledge, the authors propose using the EC4 Annex H approach [4] to calculate the structural resistance at elevated temperature, and thus calculate the steel limiting temperature at which the column fails, conservatively assuming that the protected CFS section in question experiences a *uniform temperature* over its entire cross-section.

To illustrate this approach, Figure 11 shows the observed and predicted temperature profiles of an example column from tests conducted at the National Research Council of Canada (NRC) [16], for both unprotected and uniform thermal profile states. This column was a 219.1 Ø × 5 mm wall thickness unprotected circular CFS column which failed after 80 minutes at a steel temperature of 924^{o}C. The column had fixed-fixed end conditions and an effective length of 2 m in the fire limit state; it was a 350 MPa steel tube filled with 31 MPa concrete. This resulted in a design load capacity of 1399 kN according to EC4 Annex H. The applied load during the test was 492 kN giving a load ratio of 0.35. This column was similar in dimensions to the 219.1 Ø x 5 mm columns of the current study.

Figure 11 shows that the steel temperature at 80 minutes for the unprotected 219.1 Ø x 5 mm column presented in Table 1 was 75^{o}C lower than that observed in the example test, however, the thermal gradient within the concrete core of the NRC column would be similar to that observed in the current study for the unprotected CFS section since the steel temperatures observed in both cases are similar. Figure 11 also shows the significantly shallower thermal gradient in the protected 219.1 Ø x 5 mm column at 120 minutes (recall that the design fire resistance was 90 minutes to an assumed steel tube limiting temperature of 520^{o}C).

If the example column required protection using an intumescent coating so as to increase its fire resistance, then the thermal profile of the concrete core, due to the intumescent coating, would become shallower. If one designed the intumescent coating based on the limiting temperature found for the unprotected case (i.e. 924^{o}C) then the concrete core would have a considerably higher average temperature when the limiting temperature is reached and the column would fail *before* achieving the required fire resistance. However if one calculated the limiting temperature using the EC4 Annex H approach [4] and assumed that the column had a uniform cross-section temperature, the critical failure temperature for

the steel would be about 625^{o}C (about 300^{o}C less than in the unprotected case). In reality such an approach will always be conservative since a thermal gradient within the concrete will be present and the concrete core will generally have more strength than assumed using the proposed method; this is the method recommended by the authors for the time being.

5 Conclusions

This paper has presented selected results from standard furnace tests on 14 protected and 12 unprotected CFS sections with intumescent fire protection. Based on analysis of the test data and comparison against available design guidance, the following conclusions can be drawn:

- The current method of prescribing intumescent coating DFTs for CFS sections is overly conservative for the products tested herein. The design limiting steel temperatures were generally not reached during testing with recorded steel tube temperatures of the 14 protected CFS sections some 250^{o}C less than the designed limiting temperature of 520^{o}C at the required fire resistance time.
- This paper has proposed an improved and more physically realistic instantaneous effective section factor model for unprotected CFS sections, incorporating the effects of the size of the section and the required fire resistance time; this was developed using the same methods as the current UK fire design guidance for CFS sections. However, the paper has also shown that the time averaged effective section factors determined using the new approach made design DFTs even more conservative for protected CFS columns.
- The observed conservatism in the current approach to specify design DFTs (for the reactive coating used herein) is due to the inappropriate application of unprotected CFS effective section factors for the prescription of intumescent coatings on protected CFS sections. Until a more rational method for determining the effective section factors for protected CFS sections is developed the current guidance [8] should be used.

- The design of intumescent protection systems cannot defensibly use the limiting temperature of the steel tube at failure for an unprotected CFS column as an input parameter in design. A rational and conservative method for calculating the limiting steel tube temperature using the EC4 Annex H approach [4], with an assumed uniform section temperature, has been proposed.

6 Acknowledgements

The authors gratefully acknowledge the support of Arup (Fire Engineering), The Ove Arup Foundation, The Royal Academy of Engineering, the Engineering and Physical Sciences Research Council, and the School of Engineering at the University of Edinburgh.

7 References

[1] V. Kodur, "Guidelines for fire resistant design of concrete filled steel HSS columns: State-of-the-art and research needs," *Int. J. Steel Struct.*, vol. 7, no. 3, pp. 173–182, 2007.

[2] Communities and Local Government, "Approved Document B – Volume 2 – Buildings other than dwelling houses," London, UK, 2007.

[3] T. Lennon, D. B. Moore, Y. C. Wang, and C. G. Bailey, *Designers' guides to the Eurocodes*. London, UK: Thomas Telford Publishing, 2007.

[4] CEN, "BS EN 1994-1-2: Eurocode 4: Design of composite steel and concrete structures; Part 1-2: Structural Fire Design," Brussels, Belgium, 2005.

[5] Y. C. Wang and A. Orton, "Fire resistant design of concrete filled tubular steel columns," *Struct. Eng.*, vol. 7, no. October, pp. 40–45, 2008.

[6] J. M. Aribert, C. Renaud, and B. Zhao, “Simplified fire design for composite hollow-section columns,” in *Proceedings Of The Institution Of Civil Engineers - Structures and Buildings*, 2008, vol. 161,6, no. December, pp. 325–336.

[7] Daniel Madrzykowski and D. W. Stroup, “Basics of Fire and Fire Science: Flammability Hazard of Materials,” in in *Fire Protection Handbook*, 20th ed., NFPA, 2008, pp. 2–31:2–48.

[8] S. J. Hicks, G. M. Newman, M. Edwards, and A. Orton, “Design guide for concrete filled columns,” Corus Tubes, Corby, Northants, 2002.

[9] ISO, “ISO 834: Fire resistance tests-elements of building construction,” Geneva, Switzerland, 1999.

[10] D. Rush, “Fire performance of unprotected and protected concrete filled structural hollow sections,” University of Edinburgh, 2013.

[11] CEN, “BS EN 13381-8:2010: Test methods for determining the contribution to the fire reistance of structural members; Part 8: Applied reactive protection to steel members,” Brussels, Belgium, 2010.

[12] M. Edwards, “Reinstatment of concrete filled structural hollow section columns after short duration fires - Phase 2: Standard fire tests on full size columns.,” Corby, Northants, 1998.

[13] CEN, “BS EN 1993-1-2:2005: Eurocode 3: Design of steel stuctures; Part 1-2: General rules - Structural fire design,” Brussels, Belgium, 2009.

[14] CEN, “BS EN 1991-1-2: Eurocode 1: Actions on structures; Part 1-2: General Actions - Actions on structures exposed to fire,” Brussels, Belgium, 2009.

[15] T. Paloposki and L. Liedquist, *Steel emissivity at high temperatures - Research notes*. Tampere, Finland: Technical Research Centre of Finland, 2005.

[16] T. T. Lie and M. Chabot, “Experimental studies on the fire resistance of hollow steel columns filled with plain concrete - Internal Report No. 611,” National Research Council Canada, Ottawa, Canada, 1992.

Table 1: Specimen details and average temperatures recorded at 90 and 120 minutes of fire exposure.

No.	Size (d or b) (mm)	Wall thickness (wt) (mm)	Length (L) (mm)	F.R. (mins)	H_p/A_{eff} (m^{-1})	DFT (mm)	Temperatures (^oC)			
							Steel		Concrete	
							90 mins	120 mins	90 mins	120 mins
Unprotected specimens										
1	323.9Ø	10	1000	N/A			875	949	121	132
2	323.9Ø	8	1000				862	931	119	134
3	219.1Ø	10	1400				902	981	193	377
4	219.1Ø	8	1400				887	971	180	330
5	219.1Ø	5	1400				889	973	178	331
6	139.7Ø	10	1400				944	1005	684	844
7	139.7Ø	8	1400				925	991	737	882
8	139.7Ø (a)	5	1400				926	997	564	756
9	139.7Ø (b)	5	1400				927	996	574	754
10	300×300[a]	10	1400				886	966	116	139
							893	975		
11	120×120[a]	10	1400				913	987	698	865
							922	995		
12	120×120[a]	5	1400				895	974	556	699
							912	984		
Protected specimens										
13	323.9Ø (a)	10	1000	90	40	3.50	204	244	60	86
14	323.9Ø (b)	10	1000	90	40	3.60	206	246	57	80
15	323.9Ø	8	1000	90	42	3.48	202	238	54	76
16	219.1Ø	10	1400	90	39	3.55	210	254	107	142
17	219.1Ø	8	1400	90	41	3.50	204	275	114	136
18	219.1Ø	5	1400	90	46	3.50	230	283	109	147
19	139.7Ø	10	1400	90	44	3.53	247	320	140	170
20	139.7Ø	8	1400	90	46	3.52	259	350	180	254
21	139.7Ø	5	1400	90	50	3.53	264	366	137	169
22	139.7Ø	5	1400	90	50	3.51	234	311	141	166
23	139.7Ø	5	1400	75	52	2.00	461	603[b]	179	326
24	139.7Ø	5	1400	120	47	4.06	270	387[c]	151	192
25	300×300[a]	10	1000	90	40	3.53	193	230	57	82
							228	275		
26	120×120[a]	5	1400	90	56	3.49	241	316	169	180
							243	311		

[a] Grey highlighted cells indicate temperatures recorded at corners in square specimens.

[b] 520^{o}C was reached at 106 minutes

[c] 520^{o}C was reached at 155 minutes and the recorded temperature at 180 minutes was 611^{o}C

Table 2: Representative instantaneous $(H_p/A_{eff})'$ and $H_p/A_{eff}\,(Th)$ values at 15 minute intervals (for an unprotected 219.1 Ø × 8 mm wall thickness circular CFS).

Time (mins)	*Inst.* $(H_p/A_{eff})'$ Eq. 6	*Inst.* $H_p/A_{eff}\,(Th)$ Eq. 1
0	129.7	125.0
15	67.4	66.8
30	49.6	56.0
45	45.3	49.8
60	*51.9*	45.6
75	28.3	42.4
90	22.8	39.9
105	20.0	37.8
120	17.9	36.1

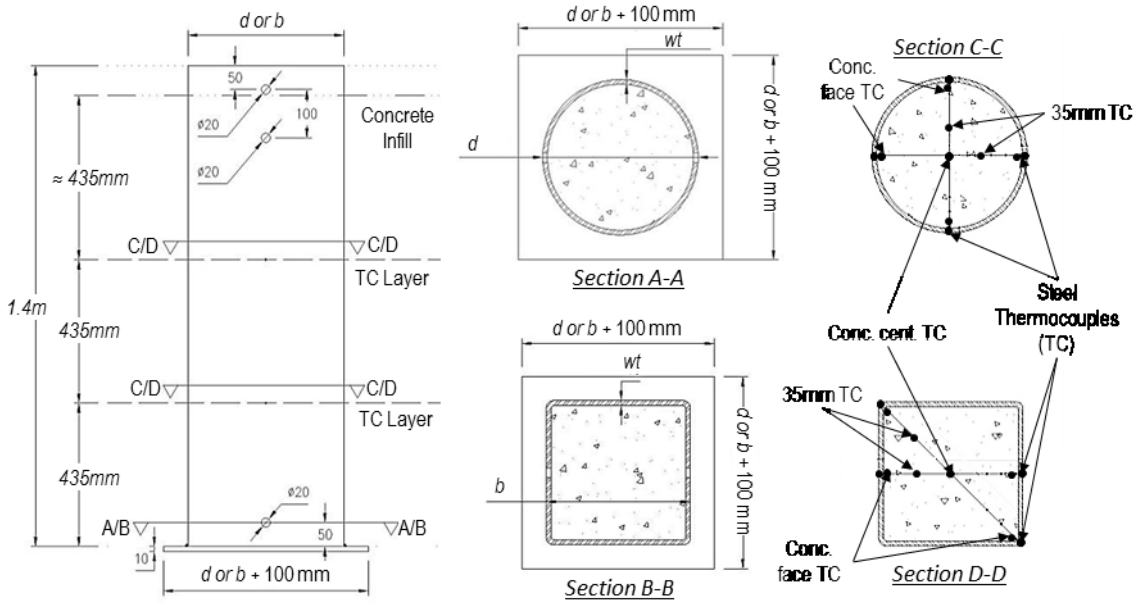

Figure 1: Specimen schematic layout

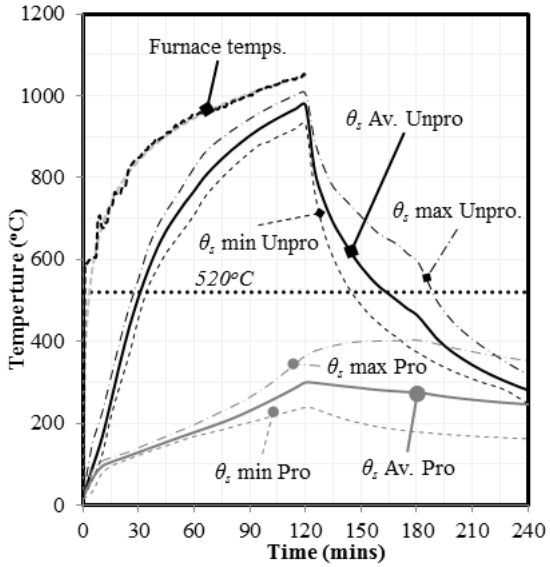

Figure 2: Comparison of unprotected and protected steel tube temperatures for CFS sections observed in furnace tests.

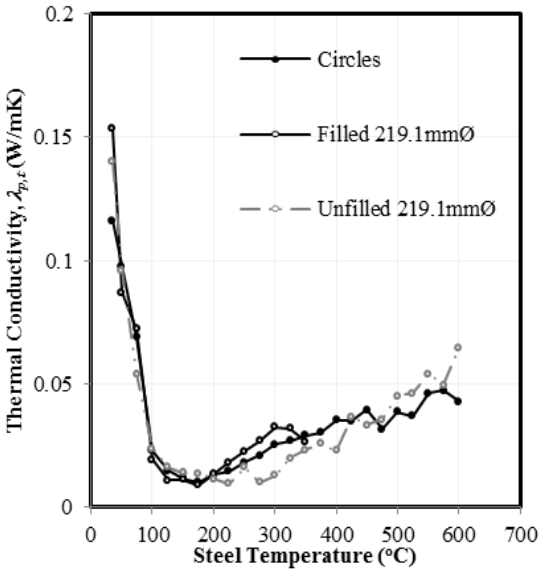

Figure 3: Comparison of variable effective thermal conductivities determined for the intumescent fire protection on filled (tests presented herein) and unfilled (test data obtained from industry partner) CFS sections.

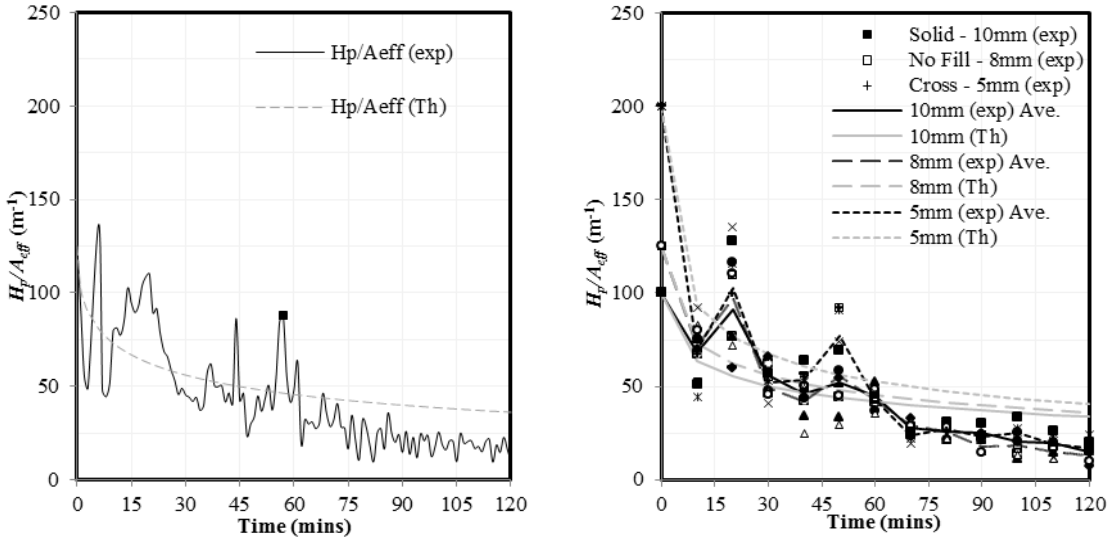

(a) (b)

Figure 4: (a) representative instantaneous H_p/A_{eff} *(exp)* and Edwards' [10] effective H_p/A_{eff} *(Th)* (for a 219.1mm Ø × 8 mm wall thickness CFS section) and (b) instantaneous effective H_p/A_{eff} *(exp)* and H_p/A_{eff} *(Th)* for all unprotected tests listed in Table 1, with the data partitioned based on steel hollow section wall thickness.

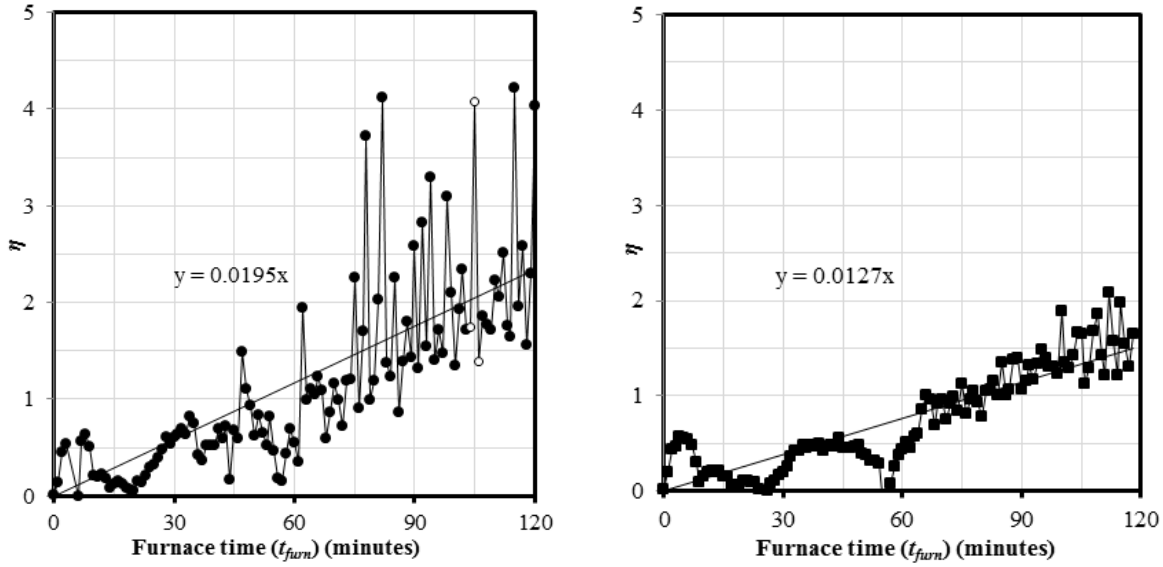

(a) (b)

Figure 5: Variation of core efficiency factor, η, with furnace exposure time, t_{furn}, with an assumed linear relationship for a typical (a) 219.1 Ø × 8 mm wall thickness circular CFS; and (b) 300 × 300 × 10 mm wall thickness square CFS.

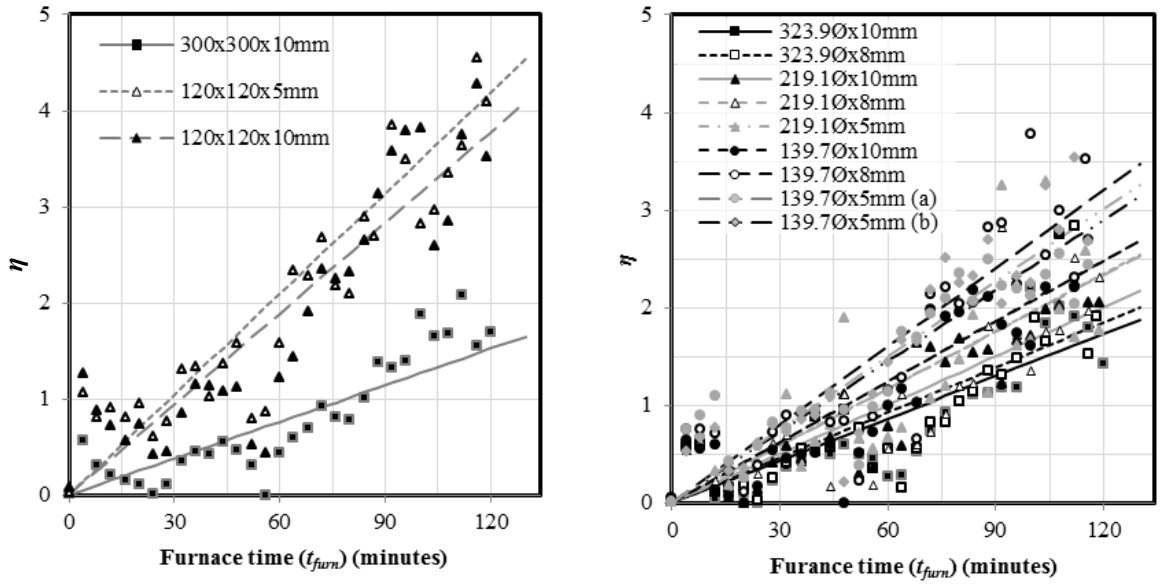

(a) (b)

Figure 6: Variation of core efficiency factor, η, with furnace exposure time, t_{furn}, for an assumed linear relationship for (a) square CFS sections; and (b) circular CFS sections.

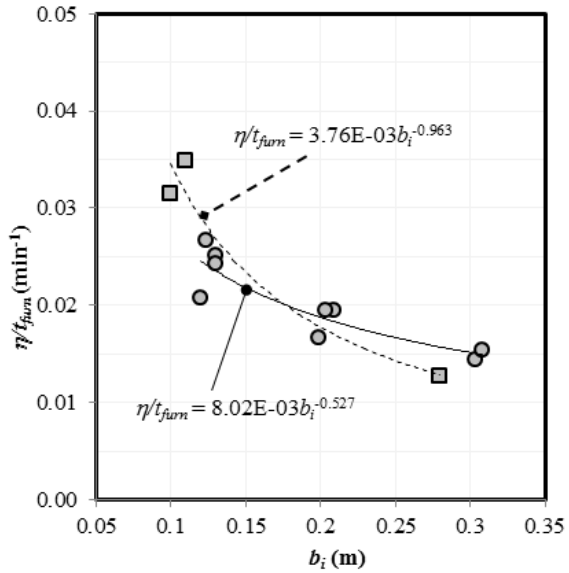

Figure 7: η/t_{furn} versus b_i relationships for square and circular CFS sections tested herein.

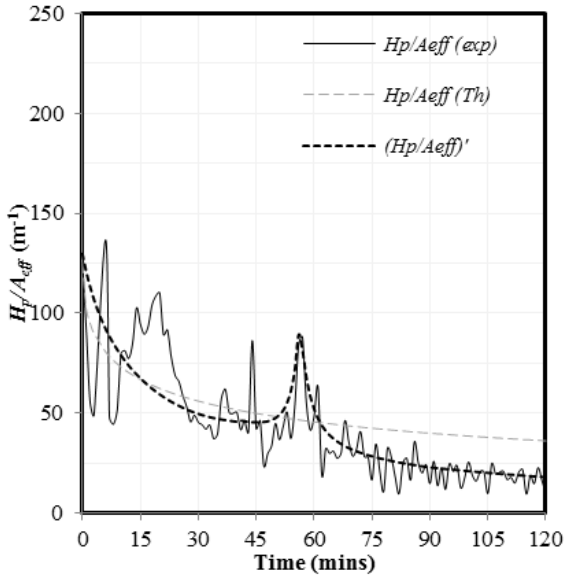

Figure 8: Comparison of $(H_p/A_{eff})'$, H_p/A_{eff} (Exp), and H_p/A_{eff} (Th) values for a representative unprotected CFS section (in this case a 219.1 Ø × 8 mm wall thickness circle).

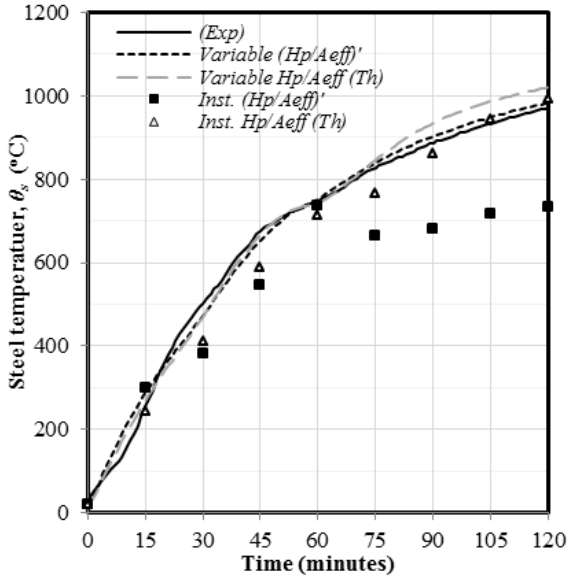

Figure 9: Representative comparison of observed and calculated steel temperatures, θ_s, using either variable or instantaneous (Inst.) values of H_p/A_{eff} (exp) and H_p/A_{eff} (Th) (for a 219.1 Ø × 8 mm wall thickness circular CFS).

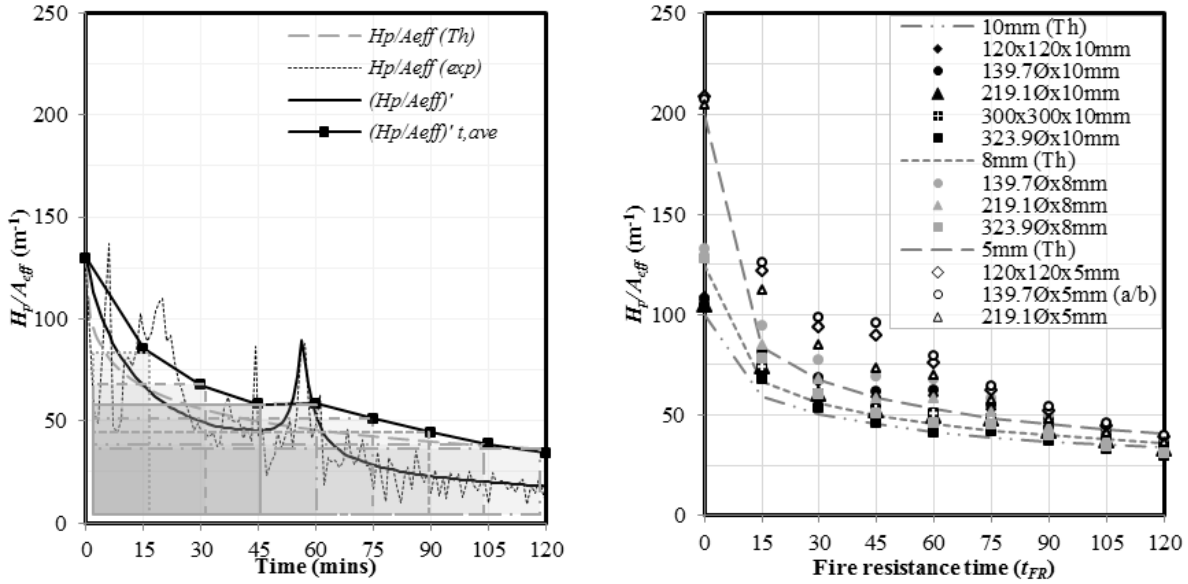

(a) (b)

Figure 10: (a) representative comparison of (H_p/A_{eff})', H_p/A_{eff} (exp), H_p/A_{eff} (Th), and $(H_p/A_{eff})'_{t.ave}$, (219.1Øx8mm); and (b) comparison of H_p/A_{eff} (Th) and $(H_p/A_{eff})'_{t.ave}$, for unprotected tests presented herein.

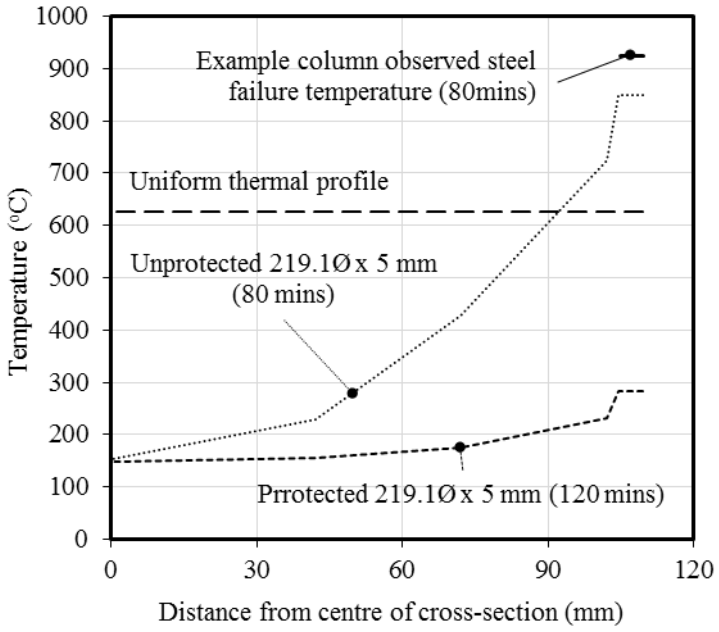

Figure 11: Representative observed temperature profiles of protected and unprotected 219.1 Ø × 5 mm circular CFS columns, and observed and predicted (using a uniform thermal profile) failure temperatures of the example column.